Reactions of Neutral Vanadium Oxide Clusters with Methanol

Feng Dong,[†] Scott Heinbuch,[‡] Yan Xie,[†] Jorge J. Rocca,[‡] and Elliot R. Bernstein*[,†]

Department of Chemistry, Department of Electrical and Computer Engineering, and NSF ERC for Extreme Ultraviolet Science and Technology, Colorado State University, Fort Collins, Colorado 80523

Received: August 25, 2008; Revised Manuscript Received: November 5, 2008

Reactions of neutral vanadium oxide clusters with methanol and ethanol in a fast-flow reactor are investigated by time-of-flight mass spectrometry. Single-photon ionization through soft X-ray (46.9 nm, 26.5 eV) and vacuum ultraviolet (VUV, 118 nm, 10.5 eV) lasers is employed to detect both neutral cluster distributions and reaction products. In order to distinguish isomeric products generated in the reactions $V_mO_n + CH_3OH$, partially deuterated methanol (CD_3OH) is also used as a reactant in the experiments. Association products are observed for most vanadium oxide clusters in reaction with methanol. Products VOD, V_2O_3D, V_3O_6D, and V_4O_9D are observed for oxygen-deficient vanadium oxide clusters reacting with methanol, while oxygen-rich and the most stable clusters can extract more than one hydrogen atom (H/D) from CD_3OH to form products $VO_2DH_{0,1}$, $V_2O_4DH_{0,1}$, $V_2O_5DH_{0,1}$, $V_3O_7DH_{0,1}$, and $V_4O_{10}DH_{0,1}$. Species $VO_2(CH_3)_2$, $VO_3(CH_3)_2$, $V_2O_5(CH_3)_2$, $V_3O_7(CH_3)_2$, and $V_3O_8(CH_3)_2$ are identified as some of the main products generated from a dehydration reaction for $V_mO_n + CH_3OH$. A minor reaction channel that generates $VOCH_2O$ ($VOCD_2O$) and VO_2CH_2O (VO_2CD_2O) can also be identified. An obviously different behavior appears in the reaction $V_mO_n + C_2H_5OH$. The main observed products for this reaction are association products of the form $V_mO_nC_2H_5OH$. In order to explore the mechanism of $V_mO_n + CH_3OH$ reactions, DFT calculations are performed to study the reaction pathways of $VO_2 + CH_3OH$ and $VO + CH_3OH$ reaction systems. The calculation results are in good agreement with the experimental observations.

I. Introduction

Transition metal oxides are important heterogeneous catalysts, and their properties and reactions have been the subject of numerous studies.[1] The oxidation of methanol is interesting because of its importance in catalytic processes;[2,3] for example, oxidative reforming of methanol is an important catalytic process in fuel cells.[4] Selective oxidation of methanol on supported vanadium oxide catalysts has been considered as a simple probe reaction for a number of other selective oxidation reactions.[5,6] The major product of methanol oxidation over V_2O_5 is found to be formaldehyde, with minor products of dimethyl ether, etc.[7] The mechanism for oxidation of methanol on supported vanadium oxide is suggested to be methanol oxidation by the catalyst, and not by gas-phase molecular O_2.[8] In this case, O_2 molecules are used to oxidize the reduced V^{4+} or V^{3+} sites back to active V^{5+} sites. In situ Raman and UV−visible measurements reveal that the catalytically active sites are fully oxidized surface VO_4 sites.[9,10] Three different V−O functionalities, terminal V═O, bridging V−O−V, and bridging V−O-support bonds, are identified for the surface of supported vanadium oxide in the catalytic methanol oxidation process.[11−13] In some studies, terminal V═O are considered to be the active sites,[14−17] and in others, bridging V−O−V are considered to be the active sites.[18] Recently, Wachs et al. suggested that the bridging V−O-support bond contributes to methanol oxidation.[3,19] Although an extensive research effort over the past two decades to explore the process of methanol oxidation in the condensed phase has been undertaken, a fundamental understanding of these catalytic reactions at an atomic and molecular level is still lacking. The complicated catalytic surface process is still difficult to interpret fully.

Gas-phase metal/metal oxide clusters and their reactions with small molecules are considered to be a model system for active sites of condensed/surface phase chemistry. Clusters generated in gas phase have relatively well-defined structures and size-dependent properties, and they are relatively accessible by theoretical calculations. A full understanding of reaction behavior of gas-phase clusters can, in principle, provide insight into the mechanism of practical catalyst systems.[20−24] The reactivity of vanadium/niobium/tantalum/zirconium oxide cluster ions toward methanol has been studied in the gas phase using mass spectrometric techniques.[21−24] The reactions of mass-selected M^+ and MO^+ (M = V, Nb, and Ta) with CH_3OH have been studied by Tang and co-workers[21] using Fourier transform ion-cyclotron resonance (FT-ICR) mass spectrometry coupled with a laser ablation ion source. In their experiments, $VO_2CH_4^+$, $VOCH_2O^+$, and VO_2^+ are detected as the main products of the reaction $VO^+ + CH_3OH$; some secondary reaction products $V(OCH_3)_2^+$ and $V(OH)_2^+$ are also observed. Employing a guided ion beam mass spectrometer, Castleman et al. studied the reactions of methanol with $V_mO_n^+$ and $Nb_mO_n^+$ cluster ions.[22] The products observed in their experiments are H_2, CH_3, CH_3OH, and C_2H_6O attached to mass-selected cluster ions. Recently, Schwarz's group[23] published a comprehensive study of $V_mO_n^+$ and $V_mO_{n-1}(OH)^+$ ($m = 1-4$, $n = 1-10$) cluster ion reactivity toward methanol using a mass spectrometric technique coupled with an electrospray ion source. Several reaction channels are identified in their experiments: abstraction of a hydrogen atom, a methyl radical or a hydroxymethyl radical, elimination of methane, and adduct formation. Formaldehyde is produced via four different pathways. In another experiment,

* Corresponding author. E-mail: erb@larmar.colostate.edu.
[†] Department of Chemistry, and NSF ERC for Extreme Ultraviolet Science and Technology.
[‡] Department of Electrical and Computer Engineering, and NSF ERC for Extreme Ultraviolet Science and Technology.

10.1021/jp807589q CCC: $40.75
Published on Web 03/11/2009

they[23] studied reactions of methanol with mass-selected V^+, VOH^+, VO^+, and VO_2^+ cations by FT-ICR mass spectrometry with an ablation ion source. Oxidation state of the metal is a key factor that determines cluster reactivity. Waters and co-workers investigated the metavanadate anion [VO_3^-] reacting toward methanol and ethanol through a combination of ion−molecule reactions and isotope labeling experiments in a quadrupole ion trap mass spectrometer. They found that VO_3^- reacts with methanol to form $VO_2(\eta^2\text{-}OCH_2)$ through the elimination of water.[25] Most gas-phase cluster reactivity studies explore the reactivity of metal oxide cluster ions with various small molecules, including methanol. Additionally, theoretical studies are employed to elucidate the mechanisms of ion−molecule reactions between metal/metal oxide cluster ions and methanol.[21,23,25−27] Partial charge transfer between metal oxide clusters and support materials (either bulk or surface) may play an important role in catalytic processes in the condensed phase. On the other hand, gas-phase studies of neutral clusters can provide useful information that can assist one in the analysis of condensed phase catalysis systems. Neutral clusters generally exhibit significantly different reactivity than ionic clusters in some reactions.[27−31]

Recently, our group has employed a new desktop, 26.5 eV/photon (46.9 nm), soft X-ray laser coupled with time of a flight mass spectrometer (TOFMS) to study gas-phase van de Waals clusters[32] and neutral metal oxide clusters and their reactions.[33] With this ionization source, all neutral cluster species and their reaction products can be ionized and detected. In the study of vanadium oxide clusters reacting with C_2 hydrocarbons, we found that the double bond of C_2H_4 can be broken by neutral oxygen-rich vanadium oxide clusters.

In the present work, reactions of neutral vanadium oxide clusters with methanol and ethanol are studied. Many reaction products are observed, and four kinds of reactions are identified by employing CH_3OH and deuterated (CD_3OH) methanol. DFT calculations are performed to study the reaction pathways of $VO_2 + CH_3OH$ and $VO + CH_3OH$ reaction systems. The mechanisms of $V_mO_n + CH_3OH$ reactions are discussed in detail and potential catalytic cycles for condensed-phase processes are suggested.

II. Procedures

A. Experiment. The reactions of neutral vanadium oxide clusters with methanol/ethanol are investigated using a time-of-flight mass spectrometer (TOFMS) coupled with single-photon ionization by a desktop 26.5 eV soft X-ray laser. Since the experimental apparatus has been described in detail elsewhere,[33] only a general outline of the experimental scheme will be presented in this report. Briefly, neutral vanadium oxide clusters are generated in a conventional laser vaporization/supersonic expansion source. A focused 532 nm laser (second harmonic of a Nd/YAG laser, 1064 nm) is employed to ablate a target of vanadium metal foil (99.7%, Aldrich) at 10−20 mJ/pulse. A mixture of 0.5% O_2 and He is used as expansion gas at 80 psig for the generation of V_mO_n neutral species. The reactant gas, formed by flowing He (99.9%, 15 psi) through a reservoir containing methanol/ethanol (CH_3OH and C_2H_5OH are spectroscopic grade, deuterated CD_3OH is 99.8 atom % D, Aldrich) at room temperature, is pulsed into the reactor tube located ∼20 mm downstream from the exit of the expansion channel. The instantaneous reactant gas mixture pressure in the reactor cell is about 1−2 torr in this setup. In this design, the fast flow reactor (70 mm length, ∅ 6 mm) is coupled directly to the cluster formation channel (40 mm length, ∅ 1.8 mm). After the fast flow reactor, the ions created in the ablation source and fast flow reactor are removed by an electric field. Vanadium oxide clusters generated from the ablation source react with reactant gases in the fast flow reactor. The design of fast-flow reactor is similar to the one adopted by Smalley et al.[34] This method is commonly used in the study of elementary reactions of ions and neutral metal clusters. The possibility of charge exchange between the ions and the much more abundant neutral species can be neglected based on the study of Kaldor et al.[34b,c] Additionally, we have demonstrated that ion−molecule reactions do not occur in our studies of V_mO_n clusters reacting with small hydrocarbons.[33a] Neutral clusters and reaction products pass through a 4 mm skimmer into the ionization region of a TOFMS (Wiley−McLauran design, R.M. Jordan Co.), where these neutral species are ionized by the slightly focused soft X-ray laser. The resolution of the mass spectrometer (Δm/m) is about 1/1000. The calibration of mass spectrum in the experiments is based on the distribution of vanadium oxide clusters. If reactant (CH_3OH, CD_3OH, or C_2H_5OH) is added into fast flow cell reactor to collide with metal oxide clusters, mass resolution will be somewhat degenerated, but it is still better than 1/500. In the present experiments, mass spectra are accumulated about 250 laser pulses.

The rotational and vibrational temperatures of VO_2 clusters have been measured to be about 50 and 700 K, respectively.[35a] The temperatures of larger clusters should be higher than smaller clusters since more formation energy is released during larger cluster formation. In our experiments, the reactant gas mixture, CH_3OH/He or CH_3CH_2OH/He, is pulsed into a fast flow cell reactor at 15 psi backing pressure. The instantaneous gas pressure in the fast flow reactor is approximately 1−2 torr when the metal oxide clusters pass through. The clusters carried by the molecular beam stay in the cell for about 50 μs (velocity of molecular beam is about 1.5 km/s, and reactor length is 70 mm). In the fast flow cell, more than one thousand collisions occur between the clusters and bath gas at a rate about 10^7/s. Therefore, most of the metal oxide clusters are cooled to room in these reactivity experiments. The concentration of alcohol is about 15% in He (backing pressure of He is 15 psi, and vapor pressure of CH_3OH is about 125 torr at 298 K). The collisions between CH_3OH and clusters are estimated at about 100 in the fast flow cell.

The soft X-ray laser (26.5 eV/photon energy) emits pulses of about 1 ns duration with an energy/pulse of 10 μJ at a repetition rate of up to 12 Hz.[36] A pair of gold-coated mirrors, a torodial and a plane mirror, is placed in a grazing incidence Z-fold configuration just before the ionization region of the TOFMS to provide alignment and focusing capabilities for the laser with respect to the molecular beam in the ionization region. The transmissivity of the Z-fold mirror system is about 40%. A large number of He^+ ions can be produced by 26.5 eV ionization of He in the molecular beam, and these could broaden the V_mO_n, etc. mass spectral features. The soft X-ray laser radiation is not tightly focused in the ionization region to avoid multiphoton ionization and a space charge Coulomb effect due to He^+ ions.

Since a 26.5 eV photon from the EUV laser is able to ionize the He carrier gas employed in the expansion, the microchannel plate (MCP) ion detector voltage is gated to reduce the MCP gain when He^+ arrives at the mass detector, in order to prevent detector circuit overload and saturation. 118 nm laser light is generated by focusing the third harmonic (355 nm, ∼30 mJ/pulse) of a Nd:YAG laser in a tripling cell that contains about a 250 torr argon/xenon (10/1) gas mixture. To separate the

generated 118 nm laser beam from the 355 nm fundamental beam, a magnesium fluoride prism (apex angle = 6°), which was not employed in our previous studies,[35] is inserted into the laser path. In this case, one is quite sure that mass signals are generated by ionization purely through the VUV laser radiation at low power (~1 μJ/pulse, pulse duration ~5 ns).

B. Theoretical Calculations. DFT calculations are carried out using the Gaussian 03 program.[37] The B3LYP functional[38] and TZVP basis set[39] are used. Vyboishchikov et al.[40] employed DFT calculations to study vanadium oxide clusters at the B3LYP/TZVP level for the first time, and then more thorough tests of this method were performed by Sauer and co-workers.[40] More recent studies of the reactivity of vanadium oxides using the B3LYP functional can be found in ref 41. The calculations are performed on two reaction systems, $VO_2 + CH_3OH$ and $VO + CH_3OH$. For each reaction channel, the calculation involves geometry optimization of various reaction intermediates and transition states. Intrinsic reaction coordinate (IRC) calculations[42,43] are also performed to confirm that a transition state connects two appropriate local minima on the reaction potential energy surface. The reaction potential surfaces (PES) plotted in the terms of zero-point-energy-corrected ΔE are thus used to explain experimental results.

III. Results

A. V_mO_n Clusters. Figure 1 displays mass spectra, generated by 26.5 eV single-photon ionization of reactants and products for the reactions of V_mO_n clusters with CH_3OH. Neutral vanadium oxide clusters are generated at low oxygen concentration conditions (0.5% O_2/He expansion). In the present paper, the formula V_mO_n is used to represent general vanadium oxide clusters. The predominant species are identified as reactants VO_2, V_2O_4, V_2O_5, V_3O_7, V_4O_{10}, V_5O_{12}, etc., as shown in the lower spectra of Figure 1, a, b, and c, for different cluster size regions. These vanadium oxide clusters have the most stable stoichiometric structures as demonstrated experimentally and theoretically.[33a,41a,b,44] A number of oxygen-deficient vanadium oxide clusters (VO, $V_2O_{2,3}$, $V_3O_{5,6}$, $V_4O_{8,9}$, $V_5O_{9,10,11}$, and $V_6O_{13,14}$) are observed in the cluster distribution. They are missing one or two oxygen atoms compared to the most stable clusters, and present a tendency to become the most stable clusters by reacting with O or O_2.[41a,b] Some oxygen-rich clusters (VO_3, V_3O_8, and V_5O_{13}, etc.) are also observed in the mass spectra. They have one or more oxygen atoms compared to the most stable clusters and present a tendency to lose O or O_2 and become the most stable clusters.[41a,b] Additionally, one can find that these oxygen-rich neutral vanadium oxide clusters are always present with one or more attached hydrogen atoms, such as VO_3H_2, $V_2O_6H_2$, $V_3O_8H_{1,2}$, etc.[33c] The TOFMS signals are often more intense than their pure V_mO_n counterpart signals. For the most stable vanadium oxide clusters (except V_2O_5), the hydrogen-containing cluster signals are smaller than 5% of the metal oxide cluster signals; and for oxygen-deficient clusters, no hydrogen-containing cluster signals are observed in the V_mO_n cluster distribution.

B. Reactions of V_mO_n Clusters with CH_3OH. To study the reactions of neutral V_mO_n clusters with methanol, mixed CH_3OH/He gas is pulsed into the reactor at a pressure of 15 psi. When the neutral vanadium oxide clusters generated from the ablation/expansion source pass through the reactor cell, collisions will occur between neutral V_mO_n clusters and CH_3OH molecules. Reaction products and the remnant neutral V_mO_n clusters are detected by a 26.5 eV laser ionization. As shown in Figure 1, several kinds of main products are identified for the reactions $V_mO_n + CH_3OH$.

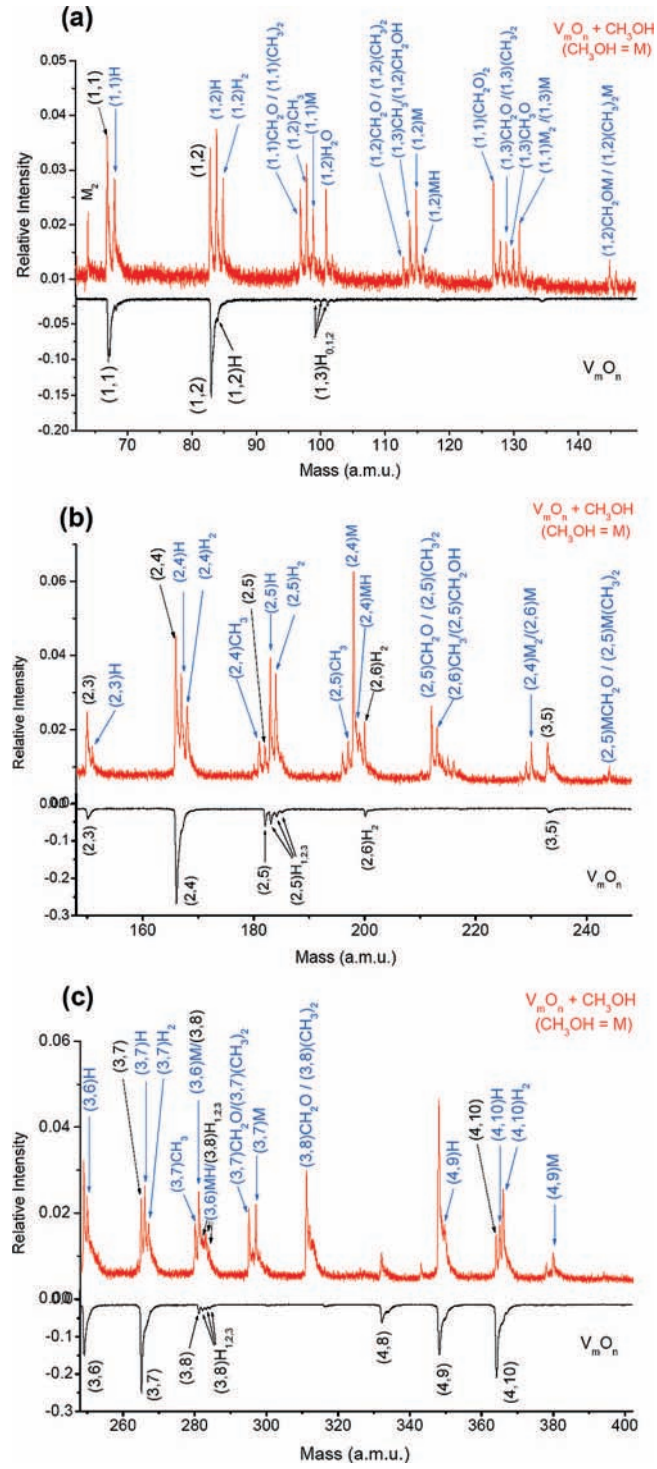

Figure 1. Reactions of V_mO_n clusters with CH_3OH studied by 26.5 eV soft X-ray laser ionization. The lower spectrum displays the V_mO_n cluster distribution generated by a 0.5% O_2/He expansion gas; the upper spectrum displays the new cluster distribution and products of the V_mO_n + CH_3OH reaction after CH_3OH/He is added to the fast flow reactor. Expanded mass regions around different size clusters are shown in (a), (b), and (c).

First, association products, $VO(CH_3OH)_{1,2}$, VO_2CH_3OH, $V_2O_4(CH_3OH)_{1,2}$, $V_3O_6CH_3OH$, and $V_3O_7CH_3OH$ etc., are observed, and they are generated from association reactions. Hydrogen transfer may occur between V_mO_n and CH_3OH in these association complexes. Second, a series of products VOH,

$VO_2H_{1,2}$, V_2O_3H, $V_2O_4H_{1,2}$, $V_2O_5H_{1,2}$, V_3O_6H, $V_3O_7H_{1,2}$, V_4O_9H, and $V_4O_{10}H_{1,2}$ is identified in the mass spectra. They can be generated by the abstraction of hydrogen atoms from CH_3OH molecules. Note that one-hydrogen-attached products VOH, V_2O_3H, V_3O_6H, and V_4O_9H are identified for oxygen-deficient clusters (VO, V_2O_3, V_3O_6, V_4O_9) reacting with methanol, while one- or two-hydrogen-attached products $VO_2H_{1,2}$, $V_2O_4H_{1,2}$, $V_2O_5H_{1,2}$, $V_3O_7H_{1,2}$, and $V_4O_{10}H_{1,2}$ are identified for the clusters with the most stable stoichiometry (VO_2, V_2O_4, V_2O_5, V_3O_7, and V_4O_{10}). Oxygen-rich vanadium oxide clusters (VO_3, V_2O_6, V_3O_8, etc.) can extract more than one hydrogen atom from methanol to form clusters, such as VO_3H_2, $V_2O_6H_2$, and $V_3O_8H_{1,2,3}$ (Figure 1). Any trace of H_2O, hydrocarbons, H_2, etc. absorbed in or on the metal, or surface OH in the experimental system can be a hydrogen source due to the high reactivity of oxygen-rich clusters, in general. The mechanisms for these reactions and the number of involved methanol molecules required for product generation are discussed below.

The third variety of products observed in $V_mO_n + CH_3OH$ reactions is $V_mO_n(CH_3OH)_{0,1}CH_2O$; for example, $VOCH_2O$, VO_2CH_2O, $VO_2(CH_3OH)CH_2O$, VO_3CH_2O, $V_2O_5CH_2O$, $V_2O_5(CH_3OH)CH_2O$, $V_3O_6CH_2O$, $V_3O_7CH_2O$, etc. These species can be generated from dehydrogenation or dehydration reactions. The product $V_mO_nCH_2O$ can also be formulated as the isobaric cluster $V_mO_n(CH_3)_2$; for example, VO_2CH_2O has the same mass number as $VO_2(CH_3)_2$, and similar isobaric pairs can be noted for $VO_3CH_2O/VO_3(CH_3)_2$, $V_2O_5CH_2O/V_2O_5(CH_3)_2$, $V_3O_7CH_2O/V_3O_7(CH_3)_2$, etc. (shown in Figure 1). They are considered to be the fourth type of product in $V_mO_n + CH_3OH$ reactions. $V_mO_n(CH_3)_2$ may be generated from a dehydration reaction between V_mO_n and two CH_3OH. Additionally, some minor products VO_2CH_3, VO_3CH_3, $V_2O_4CH_3$, and $V_3O_7CH_3$ are detected in the mass spectrum of Figure 1. We will discuss reaction mechanisms in detail in the Discussion section for these reaction products.

Methanol clusters are easily formed in the molecular beam, so a weak signal of the $(CH_3OH)_2$ dimer relative to CH_3OH signal is detected (Figure 1) when the gas mixture CH_3OH/He is pulsed into the reactor tube. The huge signal for CH_3OH is truncated by adjusting the timing of the MCP detector turn on to prevent detector circuit overload and saturation. One knows that the $(CH_3OH)_2H^+$ signal is always observed after the ionization of the neutral trimer $(CH_3OH)_3$,[34e] so no observation of protonated $(CH_3OH)_nH^+$ ($n \geq 2$) in the mass spectrum indicates that methanol clusters are not prevalent under these experimental conditions. Therefore, reactions between V_mO_n and methanol clusters can be neglected in our experiments.

The reaction of $V_mO_n + CH_3OH$ is also studied using 118 nm laser ionization. As shown in Figure 2, most of the products observed are similar to those detected by 26.5 eV ionization, with the exception of some neutral oxygen-rich vanadium oxide clusters and products with high ionization energy, such as VO_3, $V_2O_6H_2$, and $V_3O_8H_{0,1,2,3}$,[35a] that are not present in the 118 nm spectra.

Additionally, adjusting the timing between the reactant and expansion gas pulses can increase or decrease the number of collisions between V_mO_n clusters and CH_3OH molecules, resulting in a V_mO_n cluster signal increase or decrease. The reaction product signals do not significantly change relative to the remaining V_mO_n reactant cluster signals as this timing is varied.

C. Reactions of V_mO_n Clusters with CD_3OH. Clusters of equal mass (isobars) as suggested above cannot be distinguished in the mass spectra of Figure 1: $V_mO_nCH_2O$ have the same mass number as $V_mO_n(CH_3)_2$, and $VO(CH_3OH)_2$ has the same mass number as VO_3CH_3OH since the mass number of CH_3OH is equal to molecular O_2. Therefore, the reaction channels for $V_mO_n + CH_3OH$ reactions cannot be completely resolved in the mass spectra of Figure 1. In order to distinguish the isomers produced in the reactions of $V_mO_n + CH_3OH$, deuterated methanol (CD_3OH) is employed in the reaction mixture instead of CH_3OH. Figure 3, a, b, and c, presents the mass spectra obtained under the same experimental conditions as described above except CD_3OH is substituted for CH_3OH. Products $VOCD_3OH$, VO_2CD_3OH, $V_2O_4CD_3OH$, $V_3O_6CD_3OH$, and $V_3O_7CD_3OH$ are assigned to association products between V_mO_n and CD_3OH. In the experiments with CD_3OH, no significant peaks at V_2O_3H, V_3O_5H, V_3O_6H, and V_4O_9H are observed (see Figure 3b,c); VOH is, however, observed. These V_mO_nH signals can be distinguished from their neighbor V_2O_3, V_3O_5, V_3O_6, and V_4O_9 signals even though they partly overlap each other. One mass unit can readily be resolved between V_2O_4D and V_2O_4DH, V_2O_5H and V_2O_5D, $V_2O_6H_2$ and $V_2O_4CD_3OH$, etc. even though mass resolution will decrease with increasing mass number. Therefore, the signals of VOD, V_2O_3D, V_2O_4D, V_3O_5D, and V_3O_6D are identified as the major products of hydrogen-abstraction reactions for oxygen-deficient vanadium oxide clusters reacting with CD_3OH, while $VO_2H_{0,1}D$ and $VO_2H_{1,2}$, $V_2O_5H_{0,1}D$ and $V_2O_5H_{1,2}$, $V_3O_7H_{0,1}D$ and $V_3O_7H_{1,2}$, and $V_4O_{10}H_{0,1}D$ and $V_4O_{10}H_{1,2}$ are identified for stable vanadium oxide clusters reacting with CD_3OH. In addition, isotopic scrambling for reaction products can be neglected in our experiments because only products of one D attached to oxygen-deficient vanadium oxide clusters (V_2O_3D) are observed in the reaction $V_mO_n + CD_3OH$; otherwise, one should observe the products of both D and H atom attached to oxygen-deficient clusters just as reaction products observed for the most stable vanadium oxide clusters (V_2O_5H, V_2O_5D, and V_2O_5HD).

In the reactions of $V_mO_n + CH_3OH$, isobaric products $V_mO_nCH_2O$ and $V_mO_n(CH_3)_2$ have the same mass number (in Figure 1); however, they can be distinguishable as two separated products $V_mO_nCD_2O$ and $V_mO_n(CD_3)_2$ with different mass numbers for $V_mO_n + CD_3OH$ reactions. Both $OVOCD_2$ and $VO(CD_3)_2$ are observed, while only $VO_2(CD_3)_2$, $VO_3(CD_3)_2$, $V_2O_5(CD_3)_2$, $V_3O_7(CD_3)_2$, and $V_3O_8(CD_3)_2$ are observed (see

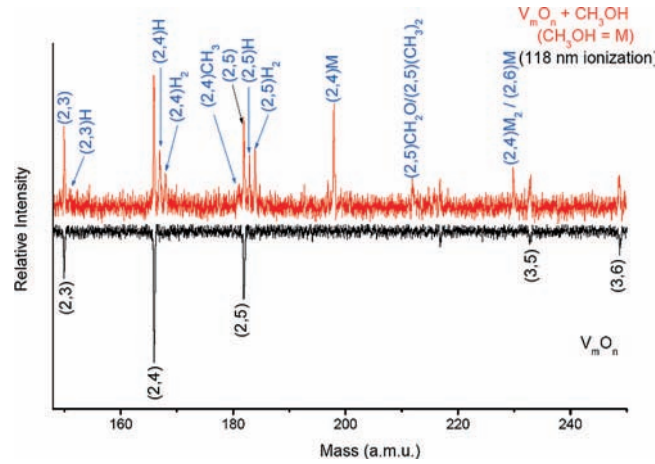

Figure 2. Reactions of V_mO_n clusters with CH_3OH studied by 118 nm (10.5 eV) laser ionization. The products detected by 10.5 eV laser ionization are similar to those detected by 26.5 eV soft X-ray laser ionization shown in Figure 1b.

Figure 3). Products $VO_2(CH_3)_2$, $VO_3(CH_3)_2$, $V_2O_5(CH_3)_2$, $V_3O_7(CH_3)_2$, and $V_3O_8(CH_3)_2$ rather than VO_2CH_2O, VO_2CH_2O, $V_2O_5CH_2O$, $V_3O_7CH_2O$, and $V_3O_7CH_2O$ are thus confirmed for the reactions $V_mO_n + CH_3OH$. $V_mO_n(CH_3)_2$ can be generated from multiple alcohol molecules reactions with V_mO_n clusters.

Assigned vanadium oxide clusters and their reaction products with CH_3OH and CD_3OH are listed in Table 1.

D. Reactions of V_mO_n Clusters with C_2H_5OH. Another alcohol compound, ethanol C_2H_5OH, is also used as a reactant with V_mO_n clusters. When C_2H_5OH/He gas is added to the reactor, many new product signals are observed in the mass spectra associated with reactions between V_mO_n and C_2H_5OH. As shown in Figure 4, the major products observed are association adducts $V_mO_n(C_2H_5OH)H_{0,1,2}$, implying that different reaction mechanisms must be responsible for V_mO_n cluster reacting with CH_3OH and reacting with C_2H_5OH.

E. DFT Calculations of $VO_2 + CH_3OH$ and $VO + CH_3OH$ Reactions. In order to explore the reaction mechanisms for the above described chemistry, we perform DFT calculation for the reaction of $VO_2 + CH_3OH$. Several possible reaction pathways are considered as follows:

$$VO_2 + CH_3OH \rightarrow HVO_2H + CH_2O \qquad \Delta H_{298} = -0.69 \text{ eV} \quad (1a)$$

$$\rightarrow HOVOH + CH_2O \qquad \Delta H_{298} = -0.60 \text{ eV} \quad (1b)$$

$$\rightarrow OVOCH_2 + H_2O \qquad \Delta H_{298} = -0.32 \text{ eV} \quad (1c)$$

$$\rightarrow VO_2CH_2 + H_2O \qquad \Delta H_{298} = +0.6 \text{ eV} \quad (1d)$$

$$\rightarrow VO_2CH_2O + H_2 \qquad \Delta H_{298} = -0.51 \text{ eV} \quad (1e)$$

Figure 5 displays the potential surface for reaction 1 and optimized geometries of reaction intermediates and transition states. Two possible channels are found for dehydrogenation reaction to generate products $CH_2O + HVO_2H$ (**P1**):

R1 → IM1 → ts1/2 → IM2 → ts2/3 → IM3 → P1 (channel Ia)

R1 → IM1 → ts1/4 → IM4_1 → ts4 → IM4_2 → ts4/3 → IM3 → P1 (channel Ib)

The reactions of VO_2 with CH_3OH start with the formation of adduct complex **IM1**, in which O atom of CH_3OH connect to V atom of VO_2. In channel Ia, first H atom transfers from OH to an O atom of VO_2 to form **IM2**, which is the most stable structure on this potential surface. The second H atom transfer from the CH_3 moiety to the V atom occurs to form **IM3** via transition state **ts2/3**. In structure **IM3**, the length of the C−V bond is increased, leading to generation of final products **P1** ($CH_2O + HVO_2H$), in which the two H atoms connect with V and O atoms. In channel Ib, the first H atom transfers from the CH_3 group to an O atom of VO_2 to form intermediate **IM4_1**, and then the structure changes to isomeric **IM 4_2**. The second H atom transfers from the OH moiety to the V atom of the VO_2 cluster to form **IM3** through transition state **ts4/3** with a small positive barrier of about 0.05 eV. Comparison of these two reaction channels, evidence that channel Ia, in which the first H atom transfers from the OH moiety to the VO_2, is more favorable than channel Ib, in which the first H atom transfers from the CH_3 moiety to the VO_2. In addition, the final product CH_2O can also dissociate to $CO + H_2$ because the energy of $CO + H_2$ is close to CH_2O; however, the dissociation barrier for the

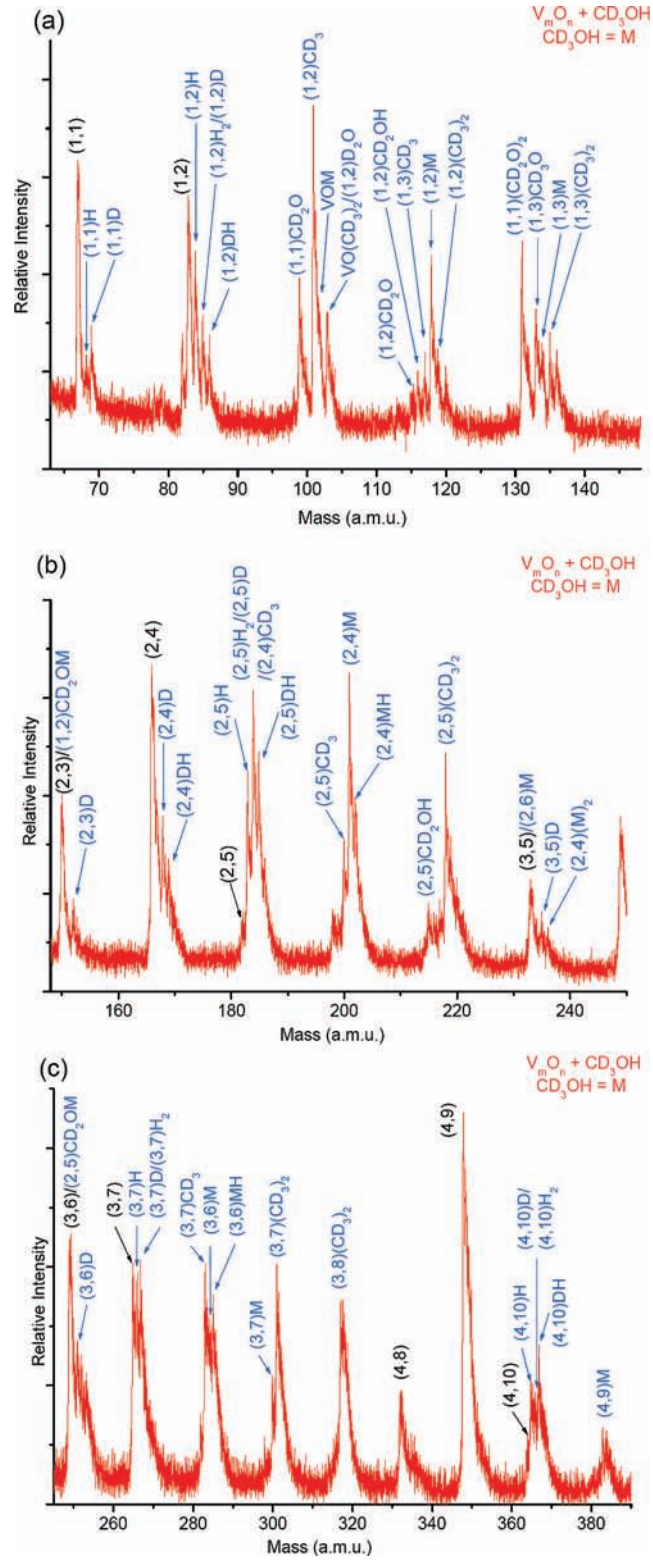

Figure 3. Reactions of V_mO_n clusters with CD_3OH studied by 26.5 eV soft X-ray laser ionization. The mass spectrum is obtained under the same experimental conditions as given in Figure 1 except that CD_3OH is substituted for CH_3OH. Expanded mass regions around different size clusters are shown in (a), (b), and (c).

TABLE 1: Observed Primary Neutral Vanadium Oxide Clusters and Their Reaction Products with CH_3OH and CD_3OH Based on Figures 1 and 3

V_mO_n	$V_mO_n + CH_3OH(M)$	$V_mO_n + CD_3OH(M)$
VO	VOH	VOH, VOD
	$VOCH_2O/VO(CH_3)_2$	$VOCD_2O$
	VOM	VOM
	$VO(CH_3)_2/VOCH_2O$	$VO(CD_3)_2$
	$VO(CH_2O)_2$	$VO(CD_2O)_2$
VO_2	VO_2H, VO_2H_2	VO_2H, VO_2D/VO_2H_2, VO_2DH
VO_2H	VO_2CH_3	VO_2CD_3
	VO_2H_2O	VO_2D_2O
	$VO_2CH_2O/VO_2(CH_3)_2$	VO_2CD_2O, $VO_2(CD_3)_2$
	VO_2CH_2OH	VO_2CD_2OH
	VO_2M, VO_2MH	VO_2M
	$VO_2CH_2OM/VO_2(CH_3)_2M$	VO_2CD_2OM
VO_3	VO_3CH_3	VO_3CD_3
VO_3H	$VO_3CH_2O/VO_3(CH_3)_2$	$VO_3(CD_3)_2$
VO_3H_2	VO_3CH_3O	VO_3CD_3O
	VO_3M/VOM_2	VO_3M
V_2O_3	V_2O_3H	V_2O_3D
V_2O_4	V_2O_4H, VO_4H_2	V_2O_4D, V_2O_4DH
	$V_2O_4CH_3$	$V_2O_4CD_3$
	V_2O_4M	V_2O_4M
	V_2O_4MH	V_2O_4MH
	$V_2O_4M_2/V_2O_6M$	$V_2O_4M_2/V_2O_6M$
V_2O_5	V_2O_5H; $V_2O_5H_2$	V_2O_5H, $V_2O_5D/V_2O_5H_2$, V_2O_5DH
$V_2O_5H_{1,2,3}$	$V_2O_5CH_3$	$V_2O_5CD_3$
	$V_2O_5CH_2O/V_2O_5(CH_3)_2$	$V_2O_5(CD_3)_2$
	$V_2O_5CH_2OH/V_2O_6CH_3$	$V_2O_5CD_2OH$
	$V_2O_5CH_2OM/V_2O_5(CH_3)_2M$	$V_2O_5CD_2OM$
$V_2O_6H_2$	$V_2O_6M/V_2O_4M_2$	$V_2O_6M/V_2O_4M_2$
V_3O_5		V_3O_5D
V_3O_6	V_3O_6H	V_3O_6D
	V_3O_6M; V_3O_6MH	V_3O_6M; V_3O_6MH
V_3O_7	V_3O_7H; $V_3O_7H_2$	V_3O_7H; $V_3O_7D/V_3O_7H_2$
	$V_3O_7CH_3$	$V_3O_7CD_3$
	$V_3O_7CH_2O/V_3O_7(CH_3)_2$	$V_3O_7(CD_3)_2$
	V_3O_7M;	V_3O_7M
V_3O_8	$V_3O_8CH_2O/V_3O_8(CH_3)_2$	$V_3O_8(CD_3)_2$
$V_3O_8H_{1,2,3}$		
V_4O_8		
V_4O_9	V_4O_9H	
	V_4O_9M	V_4O_9M
V_4O_{10}	$V_4O_{10}H$	$V_4O_{10}H$, $V_4O_{10}DH$
	$V_4O_{10}H_2$	$V_4O_{10}D/V_4O_{10}H_2$

reaction $CH_2O \rightarrow CO + H_2$ is high, ca. 90 kcal/mol (~4 eV).[42] Therefore, the reaction $VO_2 + CH_3OH \rightarrow HVO_2H + CO + H_2$ cannot occur at room temperature.

Different reaction products, **P2** (HOVOH + CH_2O), can be generated in channel II as follows,

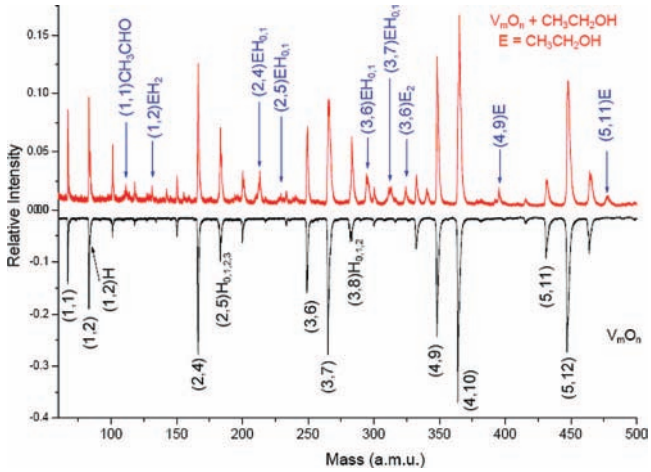

Figure 4. Reactions of V_mO_n clusters with C_2H_5OH studied by 26.5 eV soft X-ray laser ionization. The lower spectrum displays the V_mO_n cluster distribution; the upper spectrum displays the new cluster distribution and products for the reaction $V_mO_n + C_2H_5OH$ after C_2H_5OH/He is added to the fast flow reactor.

R1 → IM1 → ts1/4 → IM4_1 → ts4/5 → IM5 → ts5/6 → IM6 → P2 (channel II)

In this reaction channel, first an H atom transfers from the CH_3 to an O atom of VO_2 just as descried above for channel Ib; but the second H atom transfers from the OH to another O atom of VO_2 to form **IM5**. To form the reaction product **P2**, two H atoms bond to different two O atoms. This channel is also thermodynamically available overall barrierless at room temperature.

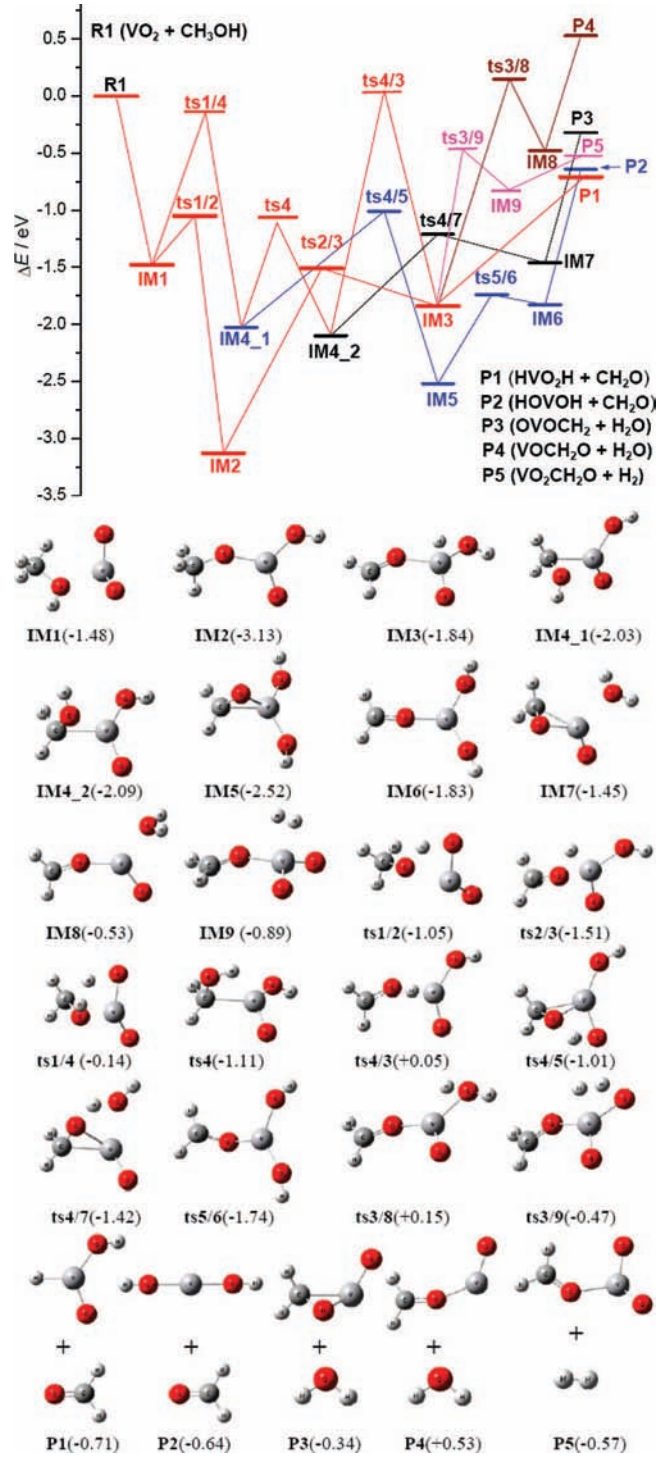

Figure 5. DFT calculated potential energy surface for the reaction $VO_2 + CH_3OH$ at the theory level B3LYP/TZVP. Structures are the optimized geometries of the reaction intermediates and transition states. Relative energies are in eV.

In the potential surface for VO_2 +CH_3OH reactions (Figure 5), two dehydration reaction channels can be calculated as follows:

R1 → IM1 → ts1/4 → IM4_1 → ts4 → IM4_2 → ts4/7 → IM7 → P3 (channel III)

R1 → IM1 → ts1/2 → IM2 → ts2/3 → IM3 → ts3/8 → IM8 → P4 (channel IV)

In channel III, the H atom of the CH_3 moiety transfers to an O atom of VO_2 for the first step. After a structural rearrangement (**IM4_1 → ts4 → IM4_2**), the second H atom transfers from the OH moiety to the same O atom to form intermediate **IM7**, in which the H_2O moiety is weakly bonded to the remainder of the cluster, finally leading to form products H_2O and $OVOCH_2$ (**P3**). In product $OVOCH_2$, an O atom is a bridge bond between V and C atoms. In channel IV, the first H atom transfers from the OH to an O atom of VO_2 without a barrier. The second H (CH_3) atom transfer has a barrier of about 0.15 eV, and the potential energy of **P4** (VO_2CH_2 + H_2O) is higher than that of initial reactants by 0.64 eV. Therefore, channel IV is a high-temperature reaction channel.

On the VO_2 cluster, a dehydrogenation reaction with CH_3OH is also overall barrierless and thermodynamically available at a room temperature as channel V in Figure 5:

R1 → IM1 → ts1/2 → IM2 → ts2/3 → IM3 → ts3/9 → IM9 → P5 (channel V)

on this pathway, the hydrogen atoms transfer from the CH_3 and OH moieties to the V atom of the VO_2 cluster, leading to form H_2 + VO_2CH_2O (**P5**) products.

The calculation for VO_2 may not be a perfect demonstration of reaction mechanisms for all the vanadium oxide clusters; however, this does indicate that the same reaction may occur on other larger stable clusters, in which VO_2 is considered a building block; such clusters include V_2O_4, V_2O_5, V_3O_7, etc. Analogous reaction products are observed in the mass spectra for these larger stable vanadium oxide clusters as well.

Calculational results indicate that hydrogen abstraction (channel I and channel II), dehydration (channel III), and hydrogen elimination (channel V) reactions are thermodynamically favorable and overall barrierless for the VO_2 + CH_3OH reaction. All these reaction products, such as VO_2H_2, $OVOCH_2$, and VO_2CH_2O, are detected in the experiments: thus, calculational results are in good agreement with experimental observations.

The potential surface on the dehydrogenation reaction between VO and CH_3OH

$$VO + CH_3OH \rightarrow VOCH_2O + H_2 \qquad \Delta H_{298} = -2.07\ \text{eV} \tag{2}$$

is explored and displayed in Figure 6. Two possible reaction channels are found as follows:

R2 → IM10 → ts10/11 → IM11 → ts11/12 → IM12 → P6 (channel VI)

R2 → IM10 → ts10/13 → IM13 → ts13/14 → IM14 → ts14/12 → IM12 → P6 (channel VII)

In channel VI, VO bonds with CH_3OH by a C−V bond to form association complex **IM10**, and then first an H atom transfers from OH to the V atom of VO to form **IM11**, which is the most stable intermediate structure on the potential surface. Second, an H atom transfers from the CH_3 moiety to the V atom again leading to **IM12** formation. Finally, H_2 leaves the complex species to generate reaction product **P6** ($VOCH_2O$ + H_2). In channel VII, first the H transfers from the CH_3 moiety to the VO to form **IM13**, and then the H atom of OH transfers to the V atom. Both channel VI and channel VII can occur overall barrierlessly at room temperature. Based on DFT calculations, the hydrogen elimination reaction between VO and CH_3OH is thermodynamically available and overall barrierless: this is consistent the experimental observation of product $OVOCH_2$ in the mass spectrum (Figures 1a and 2a).

IV. Discussion

A. Comparison between 26.5 and 10.5 eV Ionization. In the present work, a 26.5 eV (46.9 nm) soft X-ray laser is employed to ionize vanadium oxide clusters and their reaction products with methanol and ethanol. The high single-photon energy might possibly fragment/photodissociate neutral clusters or their reaction products during the ionization process and thereby confuse the identification of ground-state neutral species chemistry. In order to clarify this issue, a comparison experiment is done in which both a 10.5 and a 26.5 eV laser are used for ionization in the study of V_mO_n cluster reactions with CH_3OH.

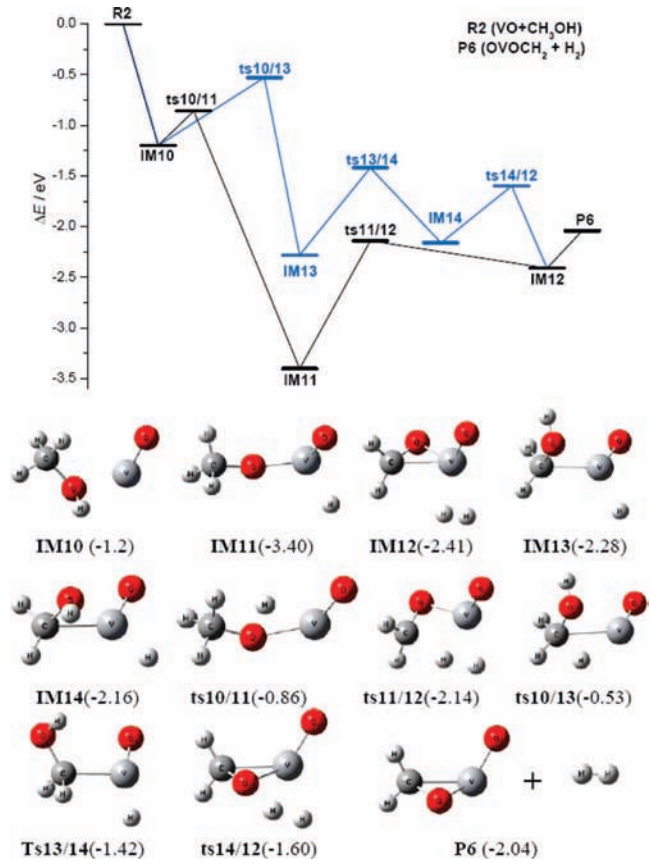

Figure 6. DFT calculated potential energy surface for the reaction VO + CH_3OH → $OVOCH_2$ + H_2 at the theory level B3LYP/TZVP. Structures are the optimized geometries of the reaction intermediates and transition states. Relative energies are in eV.

Near threshold single-photon ionization using a 10.5 eV laser photon does not leave enough excess energy in the clusters to fragment any vanadium oxide cluster or break any chemical bonds of the reaction products following ionization of the neutral species.[33] Comparing Figure 1b (26.5 eV ionization) and Figure 2 (10.5 eV ionization), one notes that the reaction products present are almost the same. Our conclusion is that the fragmentation or photodissociation of neutral vanadium oxide clusters and their reaction products caused by a single 26.5 eV photon is virtually not present in these experiments, as is well documented in ref 32a for Nb, Ta, and V samples at both 26.5 and 10.5 eV ionization energies. In our previous work, we have found that the distribution of neutral V_mO_n clusters is nearly the same using either method for ionization, with the exception that some oxygen-rich clusters with high ionization energies (>10.5 eV) cannot be detected by 10.5 eV photon ionization.[32] The reason we prefer to use 26.5 eV laser as the ionization source is that it can ionize all the neutral metal oxide clusters generated in the expansion/ablation source and all reaction products generated in the reactor. For example, $V_2O_6H_2$ is detected by a 26.5 eV laser as shown in Figure 1b but cannot be detected by a 10.5 eV laser (see Figure 2). Additionally, the signal intensity of metal oxide clusters and their reaction product is much stronger for 26.5 eV ionization than 10.5 eV ionization. 26.5 eV ionization offers more opportunities to explore large and oxygen-rich clusters and their reactions so that a general mechanism for the reactions of total cluster distribution can be explored.

B. Rate Constants for V_mO_n Clusters Reacting with CH_3OH. As shown in Figure 1, the decay fractions $(I_0 - I)/I_0$ of the V_mO_n signals in the reactions with CH_3OH are 0.3 (VO), 0.56 (VO_2), 0.66 (V_2O_4), 0.5 (V_2O_5), 0.56 (V_3O_6), 0.81 (V_3O_7), 0.38 (V_4O_9), and 0.86 (V_4O_{10}), respectively. I_0 and I are the intensities of V_mO_n signal before and after reaction with CH_3OH, respectively. The decrease of the signals caused by collisions with He and reactant CH_3OH is estimated as 50% based on the signal changes of V_2O_3, V_3O_5 clusters etc. (see Figure 1), which have almost no reactions with CH_3OH molecules. Under the experimental conditions, such as estimated CH_3OH partial gas pressure (~0.15 torr) and reaction time (~50 μs), the pseudo-first-order rate constants k ($\ln(I/I_0) = -Ckt$; C is the concentration of reactant in the reactor [22b,33a]) of $V_mO_n + CH_3OH$ reactions are calculated as 1.3×10^{-12} (VO), 3.1×10^{-12} (VO_2), 4.1×10^{-12} (V_2O_4), 2.6×10^{-12} (V_2O_5), 3.1×10^{-12} (V_3O_6), 6.3×10^{-12} (V_3O_7), 1.8×10^{-12} (V_4O_9), and 7.4×10^{-12} (V_4O_{10}) cm^3 s^{-1}. These data indicate that the stable neutral clusters VO_2, V_2O_4, V_3O_7, and V_4O_{10} are more active with CH_3OH than are the oxygen-deficient clusters VO, V_2O_3, V_3O_6, and V_4O_9. Bell and co-workers[6] experimentally and theoretically studied selective oxidation of methanol to formaldehyde on silica supported vanadium oxide. They find that the apparent activation energies for formaldehyde formation are 24.3 kcal/mol (theoretical calculation) and 23 kcal/mol (experimental measurement). The pre-exponential factors for the apparent first-order rate coefficients are 4.0×10^7 atm^{-1} s^{-1} (1.5×10^{-12} cm^3 s^{-1}) by theoretical calculation and 1.9×10^7 atm^{-1} s^{-1} (0.7×10^{-12} cm^3 s^{-1}) by experimental measurement. If one supposes no barrier ($\Delta E = 0$) for the reaction in the condensed phase, the apparent rate constant is equal to the pre-exponential factor, yielding limiting rate constant for the reaction ($k = k^0_{app} \exp(-\Delta E/RT)$; if $\Delta E = 0$, $k = k^0_{app}$). Note that for neutral V_mO_n clusters reacting with CH_3OH obtained in the gas phase, the rate constants are also ~10^{-12} cm^3 s^{-1} and are similar to those found for the condensed phase.

C. Reactions of V_mO_n + CH_3OH/CD_3OH. Reactions of neutral vanadium oxide clusters with methanol in a fast-flow reactor are investigated by time-of-flight mass spectrometry coupled with single photon ionization at 26.5 eV. Several kinds of reaction channels can be identified for $V_mO_n + CH_3OH/CD_3OH$ reactions. The details of these mechanisms are discussed for each type of reaction.

Association Reactions. Association reactions are found to be one of the main reaction channels for vanadium oxide clusters reacting with methanol. Association products $V_mO_nCH_3OH$ are detected for most of the vanadium oxide clusters. These association reactions are surely stabilized by collisions in the reactor, most likely with He gas, but also other species. On the basis of our calculations as shown in Figure 5, the most stable structure for the association complex VO_2CH_3OH is the structure of intermediate **IM2**, in which one H atom transfers from the CH_3 moiety to an O atom of VO_2. For the $VOCH_3OH$ complex, the H atom transfers from the OH moiety to the V atom to form the most stable structure **IM11** (Figure 6). For the larger clusters, the structure of association products will be more complicated, so we simply use $V_mO_nCH_3OH$ to represent the association reaction products.

As shown in Figure 1, complexes $VOCH_3OH$, VO_2CH_3OH, $V_2O_3CH_3OH$, $V_2O_4CH_3OH$, $V_3O_6CH_3OH$, $V_3O_7CH_3OH$, etc. are observed as products of the reaction of $V_mO_n + CH_3OH$. In the reaction with unlabeled methanol CH_3OH, the mass difference $\Delta m = 32$ can correspond to CH_3OH or O_2 in the mass spectrum. For example, $V_2O_4CH_3OH$ can also be assigned to V_2O_6; however, these isobars can be distinguished in the reaction of V_mO_n with deuterium-labeled methanol CD_3OH. Under the present experimental conditions, almost all V_mO_n clusters can associate with methanol to form $V_mO_nCH_3OH$. In addition, we also find that methanol molecules do not associate with neutral Zr_mO_n oxide clusters.[33b] Moreover, methanol molecules only tend to associate with the most stable and oxygen-rich Nb_mO_n and Ta_mO_n clusters, unlike for the present case in which almost all V_mO_n cluster tend to associate with CH_3OH. These experimental results suggest that methanol molecules can be readily adsorbed on neutral vanadium oxide clusters. These experimental results imply that, in the condensed phase, methanol molecules will be readily adsorbed onto the surface of a vanadium oxide catalyst and that this behavior is not necessarily universal with respect to all surfaces and/or molecules.

Hydrogen Abstraction Reactions. The abstraction of hydrogen atoms from CH_3OH to form $V_mO_nH_{1,2}$, occurs for almost all neutral vanadium oxide clusters as shown in Figure 1. Note that products with only one H atom (VOH, V_2O_3H, V_3O_6H, and V_4O_9H) are observed for oxygen-deficient clusters (VO, V_2O_3, V_3O_6, and V_4O_9), while products with one or two H atoms ($VO_2H_{1,2}$, $V_2O_4H_{1,2}$, $V_2O_5H_{1,2}$, $V_3O_7H_{1,2}$, and $V_4O_{10}H_{1,2}$) are observed for the most stable clusters (VO_2, V_2O_4, V_2O_5, V_3O_7, and V_4O_{10}).

Abstraction of two H atoms from CH_3OH will lead to a CH_2O (formaldehyde) product. Unfortunately, we cannot detect the neutral CH_2O product in our experiments since a strong CH_2O^+ signal appears in the mass spectrum due to photodissociation of CH_3OH by the 26.5 eV photons. Hydrogen abstraction reactions involve C−H and/or O−H cleavage of CH_3OH. The reaction mechanisms can be revealed in labeling experiments with CD_3OH since the cleavage of C−D or O−H will yield distinguishable products through mass spectrometry. For the reaction products $V_mO_nH_2$, two hydrogen atoms may be abstracted from one or two methanol molecules. Of course, the same issues arise for mass-selected cluster ion reactions in a

fast-flow reactor. Based on DFT calculations, the reaction for VO_2 abstracting two hydrogen atoms from two methanol molecules is not thermodynamically favorable,

$$VO_2 + 2CH_3OH \rightarrow VO_2H_2 + 2CH_2OH/OCH_3O \qquad \Delta H_{298} = +2.6\ \text{eV}/2.9\ \text{eV} \quad (3)$$

Therefore, for V_mO_n clusters, the abstraction of two hydrogen atoms from two methanol molecules should not be a major concern for the present study.

Figure 5 displays the mechanism for a hydrogen abstraction reaction between VO_2 and CH_3OH (reaction 1) generated through DTF calculations. Calculational results indicate that, for the stable cluster VO_2, abstraction of two H atoms from CH_3OH is a thermodynamically favorable reaction that is overall barrierless as shown in channel I. Hydrogen-transfer processes have no barrier no matter which H atom of CH_3 or OH moiety transfers first. For the oxygen-deficient cluster V_2O_3, abstraction of two H atoms from the CH_3OH molecule (reaction 4) is not a thermodynamic available reaction at room temperature:

$$V_2O_3 + CH_3OH \rightarrow V_2O_3H_2 + CH_2O \qquad \Delta H_{298} = +0.44\text{eV} \quad (4)$$

Therefore, the reaction products VO_2HD, V_2O_5HD, V_3O_7HD, etc. are observed for stable vanadium oxide clusters (VO_2, V_2O_5, V_3O_7, etc.), but no products V_2O_3HD, V_3O_6HD etc. are observed for oxygen-deficient clusters (V_2O_3, V_3O_6, etc.).

As shown in Figure 3 for oxygen-deficient clusters, observed products of hydrogen abstraction reactions are dominated by VOD, V_2O_3D, and V_3O_6D etc., employing CD_3OH in labeling experiments. This indicates that the abstracted hydrogen is derived from the CD_3 moiety of CD_3OH, and the concomitant product is CD_2OH. For the most stable vanadium oxide clusters, the products VO_2H, VO_2D, VO_2HD, V_2O_4H, V_2O_4D, V_2O_4HD, V_2O_5H, V_2O_5D, V_2O_5HD, V_3O_7H, V_3O_7D, V_3O_7HD, $V_4O_{10}H$, $V_4O_{10}D$, and $V_4O_{10}HD$ are observed in labeling experiments, revealing that abstracted hydrogen atoms come from both CD_3 and OH units of methanol even though the O−H bond (104.4 kcal/mol[45]) is stronger than the C−H bond (94 kcal/mol[45]). Note that the signal intensities for VO_2H, V_2O_5H, and V_3O_7H are close to those for VO_2D, V_2O_5D, and V_3O_7D, while only V_2O_3D, V_3O_5D, and V_3O_6D signals are observed (Figure 3, CD_3OH experiment). This implies that these hydrogen abstraction reactions are controlled by a dynamic mechanism on the reaction potential energy surface and not by a kinetic or statistical process, governed by the concentration ratio of D to H in CD_3OH.

Based on our calculations, abstracting one H atom from the CH_3OH molecule is not a thermodynamically available reaction for VO_2 or V_2O_3 clusters at room temperature,

$$VO_2 + CH_3OH \rightarrow VO_2H + OCH_3 \qquad \Delta H_{298} = +1.47\ \text{eV} \quad (5a)$$

$$V_2O_3 + CH_3OH \rightarrow V_2O_3H + OCH_3 \qquad \Delta H_{298} = +1.35\ \text{eV} \quad (5b)$$

Note that some $V_mO_nCH_3$ products are observed in the mass spectra, for example, VO_2CH_3 (VO_2CD_3), $V_2O_4CH_3$ ($V_2O_4CD_3$), $V_2O_5CH_3$ ($V_2O_5CD_3$), and $V_3O_7CH_3$ ($V_2O_5CD_3$). These products may be generated from the reactions of

$$2V_mO_n + CH_3OH \rightarrow V_mO_nH + V_mO_{n+1}CH_3 \quad (6a)$$

$$2V_mO_n + CH_3OH \rightarrow V_mO_{n+1}H + V_mO_nCH_3 \quad (6b)$$

Therefore, these V_mO_nH/V_mO_nD reaction products must be generated from multiple molecular reactions between V_mO_n clusters and methanol molecules. We estimate that about 100 collisions occur between a V_mO_n cluster and methanol molecules in the fast flow cell reactor. Additionally, in the studies of V_mO_n clusters reacting with methanol, we find that oxygen-deficient Nb_mO_n and Ta_mO_n clusters are not able to abstract H atom from CH_3OH to generate $Nb_mO_nH_{1,2}$ or $Ta_mO_nH_{1,2}$ products.

Oxygen-rich vanadium oxide clusters are documented to be very active in attaching H atoms from any hydrogen source (H_2O, hydrocarbons, etc.) in a high-vacuum system. Consequently, hydrogen-attached oxygen-rich vanadium oxide clusters ($V_2O_6H_{1,2}$, $V_3O_8H_{1,2}$, etc.) are always observed in the distribution of neutral vanadium oxide clusters; however, this is not true for all metal oxide clusters we have studied.[33c] The results of the present study indicate that generation of CH_2O (formaldehyde) through the abstraction of two H atoms (dehydrogenation) from one CH_3OH molecule can only occur on oxygen-rich and stable vanadium oxide clusters, and not on oxygen-deficient clusters.

The study of gas-phase cluster reactions can generate significant insight into condensed-phase elementary reaction steps (mechanisms and potential energy surfaces) for catalytic processes because clusters have relatively well-defined structures and size-dependent properties, and are readily accessible by theory. In the present study of neutral vanadium oxide cluster reactions with methanol, one finds: (1) the oxygen-deficient V_mO_n clusters (VO, V_2O_3, V_3O_6, V_4O_9) can abstract only one hydrogen atom from CH_3OH molecules to form V_mO_nH (VOH, V_2O_3H, V_3O_6H, etc.) products; (2) the stable V_mO_n clusters (VO_2, V_2O_4, V_2O_5, V_3O_7, V_4O_{10}) can abstract more than one hydrogen atom from CH_3OH to form $V_mO_nH_{1,2}$ products; and (3) oxygen-rich V_mO_n clusters (VO_3, V_2O_6, V_3O_8, etc.) can abstract more than one H atom from any hydrogen source in a high-vacuum system. DTF calculations show that for the VO_2 cluster, abstraction of two H atoms from CH_3OH to generate the formaldehyde product is thermodynamically favorable and overall barrierless; nonetheless, such a reaction is not thermodynamically available for the oxygen-deficient cluster V_2O_3 (reaction 4). Experimental and theoretical results suggest that, in the condensed phase, an oxygen-rich surface of a vanadium oxide catalyst will be able to generate a formaldehyde (H_2CO) product.

Methanol is one of the most important chemical intermediates used in industrial chemistry. Formaldehyde (H_2CO) is the major product in selective oxidation of methanol on supported vanadium oxide catalysts.[5,6] A catalytic cycle of CH_3OH oxidation to H_2CO and H_2O on VO_2 can be suggested based on our experiments and theoretical calculations. Thus, even though these gas-phase results are not necessarily specific to a complete reaction cycle, one can still suggest a mechanism for a catalytic condensed-phase process, as presented in Scheme 1.

In this catalytic cycle, the first step is the abstraction of two H atoms from CH_3OH by a VO_2 cluster or site to form products H_2CO (formaldehyde) and HVO_2H (reaction 1a). On the basis of our calculations, this process is a thermodynamically favorable and without a barrier (channel I and channel II, Figure 5). The reaction product HVO_2H is observed in mass spectrum

SCHEME 1

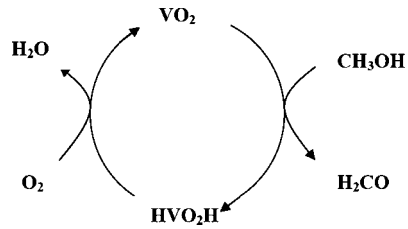

obtained for the V_mO_n + CH_3OH reaction (see Figures 1 and 3). In the second step of this cycle, the regeneration part of the cycle, the intermediate HVO_2H is oxidized by O_2 to generate products H_2O and VO_2 as given in the exothermic reaction

$$HVO_2H + \frac{1}{2}O_2 \rightarrow VO_2 + H_2O \qquad \Delta H_{298} = -1.3 \text{ eV} \tag{7}$$

The overall reaction of methanol oxidation by O_2 is thermodynamically available at room temperature:

$$CH_3OH + O_2 \rightarrow H_2O + CH_2O \qquad \Delta H_{298} = -1.6 \text{ eV} \tag{8}$$

In this catalytic cycle, methanol is selectively oxidized to formaldehyde by a VO_2 cluster. Since the same reaction products $V_mO_nH_2$ are detected for other large, stable vanadium oxide clusters such as V_2O_4, V_2O_5, V_3O_7, etc., we deduce that the catalytic cycle for VO_2 will be available for all large, stable vanadium oxide clusters, and thus for the condensed phase for which such sites or surfaces may exist.

As pointed out above, the VO_2 + CH_3OH reaction is thermodynamically favorable and overall barrierless based on our DFT calculations and experimental observations. Nonetheless, a significant barrier exits for selective oxidation of methanol on the supported vanadium oxide catalysts.[6] Generation of formaldehyde through methanol oxidation on a vanadium oxide surface is a high-temperature reaction (>600 K). One can consider two reasons for this difference between the behavior of gas-phase clusters and condensed phase surfaces: (1) the metal oxide clusters generated in the gas phase can be considered more active radicals than condensed-phase surface species; (2) at high temperature, interaction between metal oxide molecules and the metal oxide and support materials results in more active sites in terms of oxygen-deficient and oxygen-rich sites and species. Additionally, the condensed-phase studies suggest that V^{4+} and V^{5+} sites are more active than V^{3+} sites on the surface.[3] Thus, both gas-phase clusters and condensed-phase surface studies suggest that an oxygen-rich rather than an oxygen-deficient surface of a vanadium oxide catalyst will be favorable for generation of a formaldehyde (H_2CO) product.

Dehydration and Dehydrogenation Reactions. As displayed in Figure 1, a series of new products is observed in the reactions between vanadium oxide clusters with CH_3OH. Each specific mass channel corresponds to two possible isobaric products: $VO_2CH_2O/VO_2(CH_3)_2$, $VO_3CH_2O/VO_3(CH_3)_2$, $V_2O_5CH_2O/V_2O_5(CH_3)_2$, and $V_3O_7CH_2O/V_3O_7(CH_3)_2$, etc. These products are distinguished by isotopic labeling experiments ($CD_3 \leftrightarrow CH_3$). As shown in Figure 3, $VO(CD_3)_2$, $VO_2(CD_3)_2$, $VO_3(CD_3)_2$, $V_2O_5(CD_3)_2$, $V_3O_7(CD_3)_2$, etc. are assigned as the dominant products, while only $OVOCD_2$ and O_2VCD_2O are observed at the low-mass region. These products can be generated from dehydration or dehydrogenation reactions through multiple molecular reactions; for example

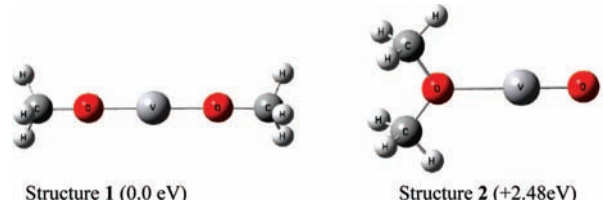

Figure 7. DFT calculation of the structures of $VO_2(CH_3)_2$. In structure **1**, two CH_3 moieties are connected to two O atoms. In structure **2**, two CH_3 moieties are connected to one O atom. Structure **1** is more stable than **2** by 2.48 eV.

$$V_mO_n + 2CD_3OH \rightarrow V_mO_n(CD_3OH)_2 \rightarrow V_mO_{n+1}(CD_3)_2 + H_2O \tag{9a}$$

$$V_mO_{n-1} + 2CD_3OH \rightarrow V_mO_{n-1}(CD_3OH)_2 \rightarrow V_mO_{n+1}(CD_3)_2 + H_2 \tag{9b}$$

The results of the labeling experiments demonstrate that eliminated H_2O or H_2 in reactions 9a and 9b are taken from OH units of two CD_3OH molecules, suggesting that two CD_3OH molecules are first adsorbed on the appropriate vanadium oxide clusters, and then a dehydration (reaction 9a) or dehydrogenation (reaction 9b) reaction occurs involving two CD_3OH molecules. Product H_2O is obtained from the OH moieties of two CH_3OH molecules, since all deuterium atoms are left on the clusters to generate $V_mO_n(CD_3)_2$. In the study of mass-selected $V_mO_n^+$ clusters,[22,23a] products $V_mO_{n-1}(CD_3O)_2$ are observed for $V_mO_n^+$ clusters.

Dehydration of CH_3OH on vanadium oxide clusters must be very fast because almost no association products with two CH_3OH/CD_3OH molecules are observed in the mass spectrum, even though dehydration products $V_mO_n(CD_3)_2$ are detected for most clusters reacting with CD_3OH. The structure of $VO_2(CH_3)_2$ is calculated as shown in Figure 7. In structure **1**, two CH_3 moieties are connected to two O atoms, respectively. This is more stable than structure **2**, in which two CH_3 moieties are connected to one O atom. For large $V_mO_n(CD_3)_2$, the structures are more complicated; however, we suggest that the structure with two CH_3 moieties are connected to two O atoms of V_mO_n will be the lowest-energy structure. Additionally, a secondary reaction, $V_mO_nCH_2O$ + $CD_3OH \rightarrow V_mO_nCH_2O(CH_3OH)$, occurs so that products $VO_2CH_2O(CH_3OH)$ and $V_2O_5CH_2O(CH_3OH)$ are observed in the experiments.

In order to explore the mechanism of dehydration and dehydrogenation reactions of methanol on V_mO_n clusters, DFT calculations are performed to study the reactions of VO and VO_2 clusters with CH_3OH. Products $OVOCH_2$ ($OVOCD_2$) and O_2VOCH_2 (O_2VOCD_2) are observed in the reactions of V_mO_n clusters with methanol as shown in Figures 1a and 3a. Product $OVOCH_2$ can be generated from two possible reactions: dehydration (1c) and/or dehydrogenation (2). Based on DFT calculations, both dehydration on the VO_2 cluster (reaction 1c) and dehydrogenation on the VO cluster (reaction 2) are thermodynamically available and overall barrierless (see Figures 5 and 6). The structure of $OVOCH_2$ can be found in **P3** and **P6**. The dehydrogenation reaction of CH_3OH is also favorable on VO_2 clusters as channel V. We suggest that dehydrogenation reactions of CH_3OH on V_mO_n clusters are thermodynamically favorable and overall barrierless. Note that CH_3OH dissociation

to generate CH_2O and H_2 is an endothermic reaction with a barrier of 3.9 eV.[46]

Comparison between V_mO_n Neutral and Ionic Cluster Reactions with CH_3OH. A comprehensive investigation of $V_mO_n^+$ cluster ion reactivity toward methanol has recently been reported by the Schwarz group.[23] Association reactions, dehydrogenation reactions to generate formaldehyde, elimination reactions to form water and hydrogen, etc. are identified based on observation of reaction products. All these reactions and products for the $V_mO_n^+$ cluster ions are also observed for the neutral V_mO_n cluster reactions with methanol in the present study. In the cluster ion studies, ref 23a reports that high-valent $V_mO_n^+$ (VO_2^+, $V_2O_4^+$, $V_3O_{6,7}^+$, $V_4O_{10}^+$) clusters are more reactive with respect to formaldehyde formation than are the lower valent cluster ions (VO^+, $V_2O_{2,3}^+$, $V_3O_{4,5}^+$, $V_4O_{7,8,9}^+$). Similar behavior is also observed for neutral V_mO_n cluster reactions with CH_3OH: abstraction of two H atoms from CH_3OH to form formaldehyde only occurs on the clusters VO_2, V_2O_4, V_2O_5, V_3O_7, and V_4O_{10}, but does not occur on the clusters VO, V_2O_3, $V_3O_{5,6}$, $V_4O_{8,9}$, etc. In addition, ref 23a finds that H_2 elimination reactions to generate $V_mO_nCH_2O^+$ products only occur for small $V_mO_n^+$ cluster ions (VO^+, VO_2^+, etc.), similar to the present study findings that the reaction products VO_2CD_2O and $VOCD_2O$ are the only detected ones for the $V_mO_nCH_2O$ product generation. Some other products detected for the neutral V_mO_n clusters reacting with CH_3OH are different from the $V_mO_n^+$ cluster ion reactions, such as V_mO_nH, $V_mO_n(CH_3)_2$, etc., which are generated from multiple molecular reactions between neutral V_mO_n clusters and methanol molecules in the fast flow reactor. Specific neutral clusters cannot be selected to react with chosen reactants, as done for cluster ion studies. Rate constants for $V_mO_n^+$ cluster reactions with methanol are measured to be of the order of 10^{-10} cm^3 s^{-1},[23a] which is about 10^2 times faster than those for neutral V_mO_n cluster reactions ($\sim 10^{-12}$ cm^3 s^{-1}) in the present study. Based on the DFT calculations, Sauer et al. conclude that $V_mO_n^+$ cluster ions are much more reactive toward methanol than are neutral clusters.[27]

D. Reactions of V_mO_n + CH_3CH_2OH. Ethanol (C_2H_5OH) is also used as a reactant to study the reactivity of V_mO_n clusters toward alcohols in general. As shown in Figure 3, association complexes $V_mO_nCH_3CH_2OH$ and $V_mO_n(CH_3CH_2OH)H$ are the major products of V_mO_n + CH_3CH_2OH reactions. V_mO_n-$(CH_3CH_2OH)H$ product may be generated from hydrogen atom transfer reactions between two ethanol molecules following their association with a V_mO_n cluster. Hydrogen abstraction products, such as VOH, $VO_2H_{1,2}$, V_2O_3H, $V_2O_5H_{1,2}$, etc., observed in V_mO_n + CH_3OH reactions are not observed for V_mO_n + CH_3CH_2OH reactions. Moreover, no obvious product is generated from dehydration or dehydrogenation for V_mO_n and CH_3CH_2OH reactions. A significant difference between CH_3OH and CH_3CH_2OH chemistry in reactions with V_mO_n clusters is apparent. One plausible reason for failure to observe anything but adduct formation with ethanol is that larger molecule leads to a longer lifetime of the intermediates formed, thereby allowing more efficient collisional stabilization, so that dissociation products are not observed for vanadium oxide clusters reacting with ethanol.

V. Conclusions

The reactions of neutral vanadium oxide clusters with methanol and ethanol are investigated employing 26.5 eV soft X-ray laser and 10.5 eV nm laser ionization coupled with TOFMS. In the experiments, nearly identical reaction products are detected using 26.5 and 10.5 eV laser ionizations. We conclude that neutral vanadium oxide clusters and their reaction products are not fragmented or photodissociated by 26.5 eV photons. Three major reactions are identified for V_mO_n + CH_3OH/CD_3OH:

(1) Association reactions: Association products $V_mO_nCH_3OH$ are observed for most of vanadium oxide clusters in the experiments, indicating that methanol molecules are easily adsorbed on neutral vanadium oxide clusters. In the condensed phase, the surface of a vanadium oxide catalyst should easily adsorb methanol molecules.

(2) Hydrogen abstraction reactions: Oxygen-deficient vanadium oxide clusters (VO, V_2O_3, V_3O_6, V_4O_9, etc.) can abstract only one hydrogen atom from a CH_3 unit of CH_3OH to form VOH, V_2O_3H, V_3O_6H, etc. products. The most stable vanadium oxide clusters (VO_2, V_2O_4, V_2O_5, V_3O_7, V_4O_{10}, etc.), can abstract more than one hydrogen atom from CH_3 and/or OH moiety of CH_3OH to form $V_mO_nH_{1,2}$ products. Oxygen-rich vanadium oxide clusters (VO_3, V_2O_6, V_3O_8, etc.) can abstract more than one H atom from any kind of hydrogen source in a high-vacuum system. The experimental results indicate that abstraction of two H atoms from CH_3OH to generate a CH_2O (formaldehyde) product takes place on oxygen-rich and stable vanadium oxide clusters but not on oxygen-deficient vanadium oxide clusters. DTF calculational results support experimental observations that the reaction of VO_2 + $CH_3OH \rightarrow HOVOH/HVO_2H + H_2CO$ is thermodynamically favorable and overall barrierless; however, $V_2O_3 + CH_3OH \rightarrow V_2O_3H_2 + CH_2O$ is not a thermodynamically available reaction. Experimental and theoretical results suggest that, in the condensed phase, an oxygen-rich surface of a vanadium oxide catalyst will be able to generate a formaldehyde (H_2CO) product.

(3) Dehydration reactions: Intense signals of $VO_2(CD_3)_2$, $VO_3(CD_3)_2$, $V_2O_5(CD_3)_2$, $V_3O_7(CD_3)_2$, and $V_3O_8(CD_3)_2$ are observed in the experiments, indicating that the dehydration reaction, $V_mO_n + 2CD_3OH \rightarrow V_mO_n(CD_3OH)_2 \rightarrow V_mO_{n+1}(CD_3)_2 + H_2O$, is one of the major reaction channels for the V_mO_n reactions with methanol. A concomitant product H_2O is derived from the OH moieties of two methanol molecules. Dehydration of CH_3OH on vanadium oxide clusters must be very fast because almost no association products $V_mO_n(CH_3OH)_2$ are detected in the experiments.

Additionally, products $VOCH_2O$ ($VOCD_2O$) and VO_2CH_2O (VO_2CD_2O) are observed in the reaction of V_mO_n clusters with CH_3OH (CD_3OH). They can be generated from reaction channels of dehydrogenation or dehydration. On the basis of our calculations, both of dehydration and dehydrogenation for VO + CH_3OH and VO_2 + CH_3OH reactions are thermodynamically available and without barriers at room temperature.

An obviously different behavior is observed for V_mO_n reactions with CH_3CH_2OH compared to CH_3OH. Association reactions are identified as the only major channel for the reaction of V_mO_n with CH_3CH_2OH.

Acknowledgment. This work is supported by AFOSR, the NSF ERC for Extreme Ultraviolet Science and Technology under NSF Award No. 0310717, and the National Center for Supercomputing Applications under Grant No. CHE080018N.

References and Notes

(1) (a) Fierro, J. L. G. *Metal Oxides Chemistry and Applications*; Taylor & Francis: London, 2006. (b) Thomas, C. L. *Catalytic Processes and Proven Catalysts*; Academic Press: New York, 1970. (c) Bell, A. T. *Science* **2003**, *299*, 1688. (d) Schroder, D.; Schwarz, H. *Angew. Chem., Int. Ed. Engl.* **1995**, *34*, 1973. (e) O'Hair, R. A. J.; Vrkic, A. K.; James, P. F. *J. Am. Chem. Soc.* **2004**, *126*, 12173.

(2) Herman, R. G.; Sun, Q.; Shi, C.; Klier, K.; Wang, C.; Hu, H.; Wachs, I. E.; Bhasin, M. M. *Catal. Today* **1997**, *37*, 1.

(3) Wachs, I. E. *Catal. Today* **2005**, *100*, 79.

(4) (a) Jusys, Z.; Behm, R. J. *J. Phys. Chem. B* **2001**, *105*, 10874. (b) Drew, K.; Girishkumar, G.; Vinodgopal, K.; Kamat, P. V. *J. Phys. Chem. B* **2005**, *109*, 11851.

(5) (a) Wachs, I. E.; Geo, G.; Juskelis, M. V.; Weckhuysen, B. M. *Stud. Surf. Sci. Catal.* **1997**, *109*, 305. (b) Weckhuysen, B. M.; Keller, D. E. *Catal. Today* **2003**, *78*, 25.

(6) (a) Goodrow, A.; Bell, A. T. *J. Phys. Chem. C* **2007**, *111*, 14753. (b) Bronkema, J. L.; Bell, A. T. *J. Phys. Chem. C* **2007**, *111*, 420.

(7) (a) Sambeth, J.; Gambaro, L.; Thomas, H. *Adsorp. Sci. Technol.* **1995**, *12*, 171. (b) Sambeth, J.; Centeno, M.; Paul, A.; Briand, L.; Thomas, H. Y.; Odriozola, J. *J. Mol. Catal. A* **2000**, *161*, 89. (c) Gambaro, L. *J. Mol. Catal. A* **2000**, *214*, 287.

(8) (a) Froment, G.; Bischoff, K. B. *Chemical Reactor Analysis and Design*; Wiley: New York, 1979. (b) Chio, S.; Wachs, I. E. Presented at 223rd ACS National Meeting, Orlando, FL,April 7−11, 2002; FUEL-509.

(9) Feng, T.; Vohs, J. M. *J. Catal.* **2004**, *221*, 619.

(10) Wong, G. S.; Concepcion, M. R.; Vohs, J. M. *J. Phys. Chem. B* **2002**, *106*, 6451.

(11) Das, N.; Eckert, H.; Hu, H.; Washs, I. E.; Walzer, J. F.; Feher, F. J. *J. Phys. Chem.* **1993**, *97*, 8240.

(12) Oyama, T.; Went, G. T.; Lewis, K. B.; Bell, A. T.; Somorjai, G. A. *J. Phys. Chem.* **1989**, *93*, 6786.

(13) Burcham, L. J.; Deo, G.; Gao, X.; Wachs, I. E. *Top. Catal.* **2000**, *11/12*, 85.

(14) Ai, M. *J. Catal.* **1982**, *77*, 279.

(15) Anderson, A. *J. Solid State. Chem.* **1982**, *4*, 279.

(16) Louis, C.; Tatibouet, J.; Che, M. *J. Catal.* **1988**, *109*, 354.

(17) Allison, J.; Goddard, W. *J. Catal.* **1985**, *92*, 127.

(18) Weber, R. *J. Phys. Chem.* **1994**, *98*, 2999.

(19) (a) Badlani, M.; Wachs, I. R. *Catal. Lett.* **2001**, *75*, 137. (b) Briand, L. E.; Jehng, J. M.; Cornaglia, L.; Hirt, A. M.; Wachs, I. E. *Catal. Today* **2003**, *78*, 257.

(20) (a) Xie, Y.; He, S. G.; Dong, F.; Bernstein, E. R. *J. Chem. Phys. A* **2008**, *128*, 044306. (b) Jakubikova, E.; Bernstein, E. R. *J. Phys. Chem. A* **2007**, *111*, 1333.

(21) Cao, Y.; Zhao, X.; Xin, B.; Xiong, S.; Tang, Z. *J. Mol. Struct.* **2004**, *683*, 141.

(22) (a) Justes, D. R.; Moore, N. A.; Castleman, A. W., Jr. *J. Phys. Chem. B* **2004**, *108*, 3855. (b) Johnson, G. E.; Mitric, R.; Tyo, R. C.; Nonacic-Koutecky, V.; Castleman, A. W., Jr. *J. Am. Chem. Soc.* **2008**, *130*, 13912.

(23) (a) Feyel, S.; Scharfenberg, L.; Daniel, C.; Hartl, H.; Schrolder, D.; Schwarz, H. *J. Phys. Chem. A* **2007**, *111*, 3278. (b) Engeser, M.; Schroder, D.; Schwarz, H. *Eur. J. Inorg. Chem.* **2007**, *17*, 2454. (c) Engeser, M.; Schroder, D.; Schwarz, H. *Chem. Eur. J.* **2005**, *11*, 5975.

(24) Jackson, P.; Fisher, K. J.; Willett, G. D. *Chem. Phys.* **2000**, *262*, 179.

(25) (a) Waters, T.; Wedd, A. G.; O'Hair, R. A. *J. Chem. Eur. J.* **2007**, *13*, 8818. (b) Waters, T.; Khairallah, G. N.; Wimala, S. A. S. Y.; Ang, Y. C.; O'Hair, R. J.; Wedd, A. G. *Chem. Commun.* **2006**, *43*, 4503.

(26) (a) Khaliullin, R. Z. K.; Bell, A. T. *J. Phys. Chem.* **2002**, *106*, 7832. (b) Boulet, P.; Baiker, A.; Chermette, H.; Gilardoni, F.; Volta, J. C.; Weber, J. *J. Phys. Chem. B* **2002**, *106*, 9659.

(27) Dobler, J.; Pritzsche, M.; Sauer, J. *J. Am. Chem. Soc.* **2005**, *127*, 10861.

(28) Justes, D. R.; Mitric, R.; Moore, N. A.; Bonacic-Koutecky, V.; Castleman, A. W., Jr. *J. Am. Chem. Soc.* **2003**, *125*, 6289.

(29) Futrell, J. H. *Gaseous Ion Chemistry and Mass Spectrometry*; Wiley: New York, 1986.

(30) Eller, K.; Schwarz, H. *Chem. Rev.* **1991**, *91*, 1121.

(31) Bohme, D. K.; Schwarz, H. *Angew. Chem., Int. Ed.* **2005**, *44*, 2336.

(32) (a) Dong, F.; Heinbuch, S.; Rocca, J. J.; Bernstein, E. R. *J. Chem. Phys.* **2006**, *125*, 154317. (b) Heinbuch, S.; Dong, F.; Rocca, J. J.; Bernstein, E. R. *J. Chem. Phys.* **2007**, *126*, 244301. (c) Heinbuch, S.; Dong, F.; Rocca, J. J.; Bernstein, E. R. *J. Chem. Phys.* **2006**, *125*, 154316. (d) Dong, F.; Heinbuch, S.; Rocca, J. J.; Bernstein, E. R. *J. Chem. Phys.* **2006**, *124*, 224319.

(33) (a) Dong, F.; Heinbuch, S.; Rocca, J. J.; Bernstein, E. R.; Wang, Z. C.; Deng, K.; He, S. G. *J. Am. Chem. Soc.* **2008**, *130*, 1932. (b) Dong, F.; Heinbuch, S.; Rocca, J. J.; Bernstein, E. R. *J. Chem. Phys.* **2006**, *125*, 164318. (c) Heinbuch, S.; Dong, F.; Rocca, J. J.; Bernstein, E. R. *J. Opt. Soc. Am. B* **2008**, *25*, 85.

(34) (a) Geusic, M. E.; Morse, M. D.; O'Brien, S. C.; Smalley, R. E. *Rev. Sci. Instrum.* **1985**, *56*, 2123. (b) Zakin, M. R.; Brickman, R. O.; Cox, D. M.; Kaldor, A. *J. Chem. Phys.* **1988**, *86*, 3555. (c) Zakin, M. R.; Brickman, R. O.; Cox, D. M.; Kaldor, A. *J. Chem. Phys.* **1988**, *88*, 6605. (d) Morse, M. D.; Geusic, M. E.; Heath, J. R.; Smalley, R. E. *J. Chem. Phys.* **1985**, *83*, 2293. (e) Knickelbein, M. B. *Annu. Rev. Phys. Chem.* **1999**, *50*, 79.

(35) (a) Matsuda, Y.; Bernstein, E. R. *J. Phys. Chem. A* **2005**, *109*, 3803. (b) Matsuda, Y.; Shin, D. N.; Bernstein, E. R. *J. Chem. Phys.* **2004**, *120*, 4142. (c) Shin, D. N.; Matsuda, Y.; Bernstein, E. R. *J. Chem. Phys.* **2004**, *120*, 4157. (d) Matsuda, Y.; Bernstein, E. R. *J. Chem. Phys.* **2004**, *120*, 4165.

(36) (a) Heinbuch, S.; Grisham, M.; Martz, D.; Rocca, J. J. *Opt. Express* **2005**, *13*, 4050. (b) Rocca, J. J.; Shlyaptsev, V. N.; Tomasel, F. G.; Cortazar, O. D.; Hartshorn, D.; Chilla, J. L. A. *Phys. Rev. Lett.* **1994**, *73*, 2192. (c) Rocca, J. J. *Rev. Sci. Instrum.* **1999**, *70*, 3799.

(37) Frisch, M. J.; et al. *Gaussian 03, Revision C.02*; Gaussian, Inc.: Wallingford, CT, 2004.

(38) (a) Becke, A. D. *Phys. Rev. A* **1988**, *38*, 3098. (b) Becke, A. D. *J. Chem. Phys.* **1993**, *98*, 5648. (c) Lee, C. T.; Yang, W. T.; Parr, R. G. *Phys. Rev. B* **1988**, *37*, 785.

(39) Schafer, A.; Huber, C.; Ahlrichs, R. *J. Chem. Phys.* **1994**, *100*, 5829.

(40) (a) Vyboishchikov, S. F.; Sauer, J. *J. Phys. Chem. A* **2000**, *104*, 10913. (b) Sauer, J.; Dobler, J. *Dalton Trans.* **2004**, 3116. (c) Pykavy, M.; van Wullen, C.; Sauer, J. *J. Chem. Phys.* **2004**, *120*, 4207. (d) Rozanska, X.; Sauer, J. *Int. J. Quantum Chem.* **2008**, *108*, 2223.

(41) (a) Jakubikova, E.; Rappé, A. K.; Bernstein, E. R. *J. Phys. Chem. A* **2007**, *111*, 12938. (b) Jakubikova, E. Ph.D. dissertation, May 2007. (c) Bande, A.; Luchow, A. *Phys. Chem. Chem. Phys.* **2008**, *10*, 3371. (d) Pykavy, M.; van Wullen, C. *J. Comput. Chem.* **2007**, *28*, 2252.

(42) Gonzalez, C.; Schlegel, H. B. *J. Chem. Phys.* **1989**, *90*, 2154.

(43) Gonzalez, C.; Schlegel, H. B. *J. Phys. Chem.* **1990**, *94*, 5523.

(44) Calatayud, M.; Andres, J.; Beltran, A. *J. Phys. Chem. A.* **2001**, *105*, 9760.

(45) *CRC handbook of Chemistry and Physics*, 62nd ed.; CRC Press: Boca Raton, FL, 1981−1982; p F192.

(46) Walsh, S. P. *J. Chem. Phys.* **1993**, *98*, 3163.

JP807589Q